

Charge Gaps at Fractional Fillings in Boson Hubbard Ladders

T. Ying,^{1,2} G.G. Batrouni,^{3,4,5} G.X. Tang,¹ X.D. Sun,¹ and R.T. Scalettar²

¹*Department of Physics, Harbin Institute of Technology, Harbin 150001, China*

²*Physics Department, University of California, Davis, California 95616, USA*

³*INLN, Université de Nice–Sophia Antipolis, CNRS,
1361 route des Lucioles, 06560 Valbonne, France*

⁴*Institut Universitaire de France, 103, Boulevard Saint-Michel, 75005 Paris, France and*

⁵*Centre for Quantum Technologies, National University of Singapore, 2 Science Drive 3, Singapore 117542*

The Bose-Hubbard Hamiltonian describes the competition between superfluidity and Mott insulating behavior at zero temperature and commensurate filling as the strength of the on-site repulsion is varied. Gapped insulating phases also occur at non-integer densities as a consequence of longer ranged repulsive interactions. In this paper we explore the formation of gapped phases in coupled chains due instead to anisotropies $t_x \neq t_y$ in the bosonic hopping, extending the work of Crepin *et al.* [Phys. Rev. B 84, 054517 (2011)] on two coupled chains, where a gap was shown to occur at half filling for arbitrarily small interchain hopping t_y . Our main result is that, unlike the two-leg chains, for three- and four-leg chains, a charge gap requires a finite nonzero critical t_y to open. However, these finite values are surprisingly small, well below the analogous values required for a fermionic band gap to open.

PACS numbers: 71.10.Fd, 02.70.Uu

I. INTRODUCTION

Experiments on ultracold atomic gases have opened new possibilities in the exploration of strongly correlated quantum physics¹. Most significantly, the ratio of interaction to kinetic energy can be readily tuned, something which is possible only with substantial effort in condensed matter systems, e.g. through the application of high pressure in a diamond anvil cell. The flexible nature of the optical lattices that can be generated using interfering lasers has also allowed the study of different dimensionality and dimensional crossover, as well as the systematic interpolation between different geometries in a given dimension, e.g. triangular to kagome² or square to triangular³.

In the case of bosonic systems, a key focus has been on the superfluid (SF) to Mott insulator (MI) quantum phase transition, which occurs at zero temperature and commensurate filling as the ratio of kinetic energy to on-site repulsion U is tuned⁴. The MI phase is characterized by a nonzero charge gap Δ_c : A plot of density, ρ , versus chemical potential, μ , exhibits plateaux when ρ takes on integer values. The critical interaction strength is now known to very high precision, e.g. taking the value $(t/U)_c = 0.05974(3)$ for a square lattice⁵. With longer range interactions, these plateaux can develop at non-integer fillings as well. For example, a sufficiently large near-neighbor repulsion V_1 drives a checkerboard solid order at $\rho = \frac{1}{2}$ on a square lattice⁶. Likewise, a next-near-neighbor repulsion V_2 can cause stripe ordering at the same filling. Both patterns of charge ordering are accompanied by a non-zero gap. Long range (e.g. dipolar) interactions give rise to a complex "devil's staircase" structure in $\rho(\mu)$ ^{7,8}. The number of plateaux which develop increases with system size, indicating the presence of frustration⁸. Another fascinating, and

experimentally realizable, mechanism which produces MI phases at fractional fillings is the presence of a superlattice superimposed on the optical lattice. These superlattice fractional filling MI phases are expected in one^{9–11} and two^{12,13} dimensions and in one-dimensional chains of tilted double well potentials^{14,15}.

In this paper we study the appearance of fractional filling MI plateaux in the Bose-Hubbard model on coupled chains which originate instead due only to *anisotropic hopping*,

$$\hat{\mathcal{H}} = -\mu \sum_i n_i + \frac{1}{2}U \sum_i n_i(n_i - 1) \quad (1)$$

$$-t_x \sum_i (a_i^\dagger a_{i+\hat{x}} + a_{i+\hat{x}}^\dagger a_i) - t_y \sum_i (a_i^\dagger a_{i+\hat{y}} + a_{i+\hat{y}}^\dagger a_i)$$

Here a_i^\dagger , a_i , and n_i are boson creation, destruction, and number operators on sites i of an $L_x \times L_y$ rectangular lattice. t_x and t_y are hopping parameters between sites i and neighboring sites in the \hat{x} and \hat{y} directions respectively. We will focus on "coupled chain" geometries in which $L_x \gg L_y$. U is an on-site repulsion, We shall consider here only the hard-core limit $U = \infty$. We note the absence of longer range interactions and superlattice potentials, so that the only possible mechanism for the fractional filling MI is the new one (anisotropic hopping) considered here.

As noted above, the presence of density plateaux in the ground state of the Hamiltonian, Eq. (1), is expected at commensurate filling for sufficiently large U , but otherwise a compressible SF phase is the most natural low temperature phase. In contrast, for fermions, additional band insulator plateaux can arise from the structure of the dispersion relation $\epsilon(\mathbf{k})$. For example, for a two-chain ($L_y = 2$) system $\epsilon(k_x, k_y) = -2t_x \cos k_x - t_y \cos k_y$ where k_y takes on only the two values $k_y = 0, \pi$.

This dispersion relation can equivalently be viewed as that of a single one-dimensional (1D) chain with two bands, $\epsilon(k_x) = -2t_x \cos k_x \pm t_y$. If $t_y > 2t_x$ the two bands are separated by a gap, and a plateau in $\rho(\mu)$ will occur at $\rho = \frac{1}{2}$.

Such gaps arising from the structure of $\epsilon(\mathbf{k})$ are typically to be expected only of fermionic systems, since they occur as a consequence of the Pauli principle and the complete filling of a lower energy band. In one dimension, however, hard-core ($U = \infty$) bosons (the "Tonks-Girardeau gas")¹⁶ share many similarities with fermions, via a Jordan-Wigner transformation¹⁷. Hence such band insulating behavior might be expected for hard-core bosons as well. Indeed, such 1D "bosonic band insulators" have been observed when a superlattice potential $\Delta \sum_i (-1)^i n_i$ is added to the 1D hard core boson Hubbard Hamiltonian¹¹. As in the two-chain case, a superlattice potential opens a gap in the dispersion relation which can be measured by the plateau in $\rho(\mu)$ and which is accompanied by a vanishing of the SF density ρ_s . Interestingly, these insulators are found to extend deep into the soft-core limit, where the Jordan-Wigner mapping to fermions is no longer valid.

Crepin *et al.*¹⁸ have recently studied another example of the persistence of the 1D Jordan-Wigner analogy between hard-core bosons and fermions by examining two-leg ladders. Here the possibility of particle exchange destroys the formal mapping and one might expect features of the fermionic case not to have bosonic analogs. Nevertheless, they found that in the large t_y limit the bosonic system exhibits a charge gap $\Delta = 2t_y - 4t_x + 2t_x^2/t_y$, where the first two terms are precisely the fermionic result. The last term represents an *increase* in the gap for hard-core bosons relative to fermions. In addition, for weakly coupled chains where $t_y \ll t_x$, the fermionic case would have overlapping bands and no charge gap. Yet for bosons Δ remains non-zero, although exponentially small, with $\Delta \propto e^{-\alpha t_x/t_y}$.

It is natural to consider the extension of the question of insulating behavior in bosonic systems to cases where there are more than two chains, and even to the two-dimensional limit. In this paper we present results for the charge gap and SF response of the Hamiltonian, Eq. (1), on three- and four-leg ladders. Our primary methodology is quantum Monte Carlo (QMC) simulations using the ALPS¹⁹ stochastic series expansion (SSE) code. We supplement this with density matrix renormalization group (DMRG) calculations also using the ALPS library. Our major result is that incommensurate gaps persist beyond the two leg case, although a finite, but surprisingly small, t_y seems to be required. For the three- and four-chain systems we find that even for $t_y/t_x = \mathcal{O}(1)$, gaps form at fractional fillings. As the number of chains increases, the finite critical value increases.

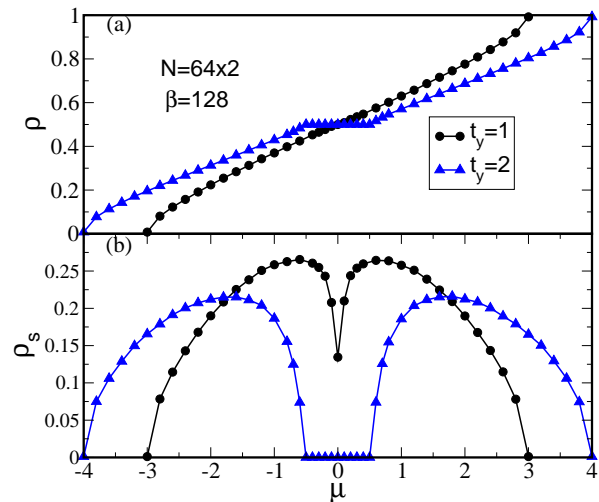


FIG. 1: (Color online) (a) $\rho(\mu)$ and (b) SF density for a 64×2 ladder of hard-core bosons with $t_x = t_y = 1$ (black) and $t_x = 1, t_y = 2$ (blue). For $t_y = 2$, a gap is visible at $\rho = \frac{1}{2}$, and the corresponding SF density vanishes, signaling the insulating state. At $t_y = 1$ the gap is not visible in the $\rho(\mu)$ plot but the dip in $\rho_s(\mu = 0)$ hints at its presence. Careful finite size scaling¹⁸ demonstrates this clearly. Here and in subsequent figures error bars are smaller than the symbol size and hence are not shown.

II. METHODOLOGY

Our simulations are performed using the SSE algorithm^{20–22}, a powerful and elegant QMC method to study quantum spin or bosonic lattice models. SSE is a generalization of Handscomb's algorithm²³ for the Heisenberg model. It starts from a Taylor expansion of the partition function in orders of inverse temperature β , and corresponds to a perturbation expansion in all terms of the Hamiltonian. There are no "Trotter errors" associated with discretization of imaginary time. We use a grand-canonical formulation of the code, but also restrict some measurements to just one particle number sector in order to generate results in the canonical ensemble.

To characterize the phases of the Hamiltonian, Eq. (1), we will examine the energy, $E = \langle H \rangle$, the variation of density as a function of chemical potential and the SF density ρ_s . The SSE code computes the SF density via the relation²⁴

$$\rho_s = \frac{\langle W^2 \rangle}{2td\beta L^{d-2}}, \quad (2)$$

where W is the winding number of the particle world lines, d is the dimensionality and β is the inverse temperature. In the coupled-chain problem we address here, we take $L_y \ll L_x$, $t_x \neq t_y$, and the boundary conditions are open (periodic) in the \hat{y} (\hat{x}) direction. Note, however, that taking periodic boundary conditions in the \hat{y} direction does not change the physics

qualitatively; the fractional filling gaps are still present but the values of the critical t_y change slightly. We focus, therefore, on the SF density in the \hat{x} direction so that the hopping parameter in Eq. (2) is t_x and the length L is L_x . In what follows, we typically take $\beta = 2L_x$ to access ground state properties. However, for small L_x where $2L_x \leq 128$, we set $\beta = 128$. In addition, for some cases of $2L_x > 128$, we verified that putting $\beta = 3L_x$ yields the same results as $\beta = 2L_x$. We also take $t_x = 1$ to set the energy scale.

III. RESULTS

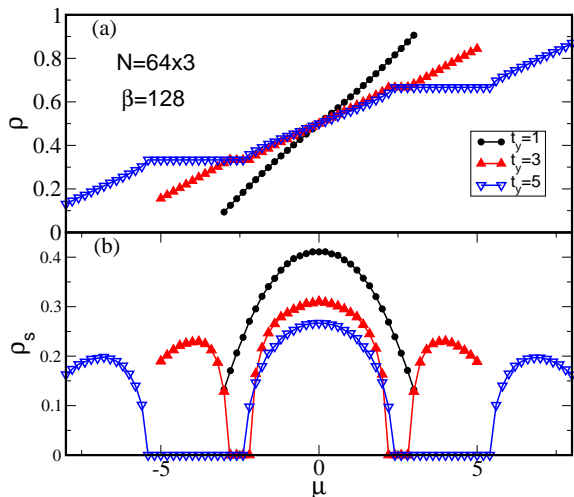


FIG. 2: (Color online) (a) $\rho(\mu)$ and (b) SF density for a three-leg ladder of hard-core bosons. As the transverse hopping t_y grows, gaps develop at $\rho = \frac{1}{3}, \frac{2}{3}$. When the chemical potential lies in the insulating gap, the SF density vanishes.

We begin by studying the two-chain case considered by Crepin *et al.*¹⁸ in order to confirm our methodology. Figure 1 demonstrates that our SSE results are fully consistent with this earlier work. A plateau in the density at half filling is clearly visible for $t_y = 2$ when $-0.5 \lesssim \mu/t \lesssim 0.5$, signaling the incompressible insulating state where the SF density vanishes. For $t_y = t_x = 1$, the plateau at half filling is not easily visible, but a sharp minimum appears in the SF density hinting at its presence. A careful finite size scaling study¹⁸ shows its presence clearly.

We now explore whether these plateaux persist in geometries having more than two chains, and if so, at what fillings. Figure 2(a) shows the density as a function of chemical potential for a three-leg ladder of 64 sites in the \hat{x} direction. Plateaux are seen to develop at $\rho = \frac{1}{3}, \frac{2}{3}$ for sufficiently large t_y . Figure 2(b) gives the SF density, and confirms that it vanishes in the gapped phase. At first glance, such incommensurate insulators might seem surprising for a model with only on-site repulsion, since

empty sites exist to which the bosons can hop without large energy cost.

As discussed already in the two-chain case, these insulators are not a surprise if the particles are fermionic: For the noninteracting system, $U = 0$, the Hamiltonian can be diagonalized by going to momentum space giving rise to the dispersion relation given in the Introduction. In the three leg case (with open boundary conditions in the \hat{y} direction), there are three bands, $\epsilon(k_x, k_y) = -2t_x \cos k_x + \{-\sqrt{2}t_y, 0, \sqrt{2}t_y\}$. For sufficiently large t_y , a gap $\Delta_f(\rho = \frac{1}{3}) = 0 - 2t_x - (-\sqrt{2}t_y + 2t_x) = \sqrt{2}t_y - 4$ is present between the top of the lowest band and the bottom of the middle band. In a fermionic model at $T = 0$ a band insulator would be present at $\rho = \frac{1}{3}$. An identical gap would appear at $\rho = \frac{2}{3}$ as a consequence of particle-hole symmetry. Thus noninteracting fermions hopping on this three chain geometry would be band insulators at $\rho = \frac{1}{3}, \frac{2}{3}$ for $t_y \geq 4/\sqrt{2} \sim 2.829$ (see Fig. 3). The gaps at large values of t_y/t_x are easy to understand in the hard core limit. When $t_x \ll t_y$, the particles delocalize much more efficiently along the \hat{y} axis, and hence spread out in that direction. Thus, when $\rho = 1/3$, the particles are in an effective one-dimensional system with a density $\rho_{\text{eff}} = 1$. This system, due to the hard core nature of the particles, becomes an incompressible insulator. This intuitive picture applies equally to the four-chain system. We examine below how small t_y should be for such behavior to change.

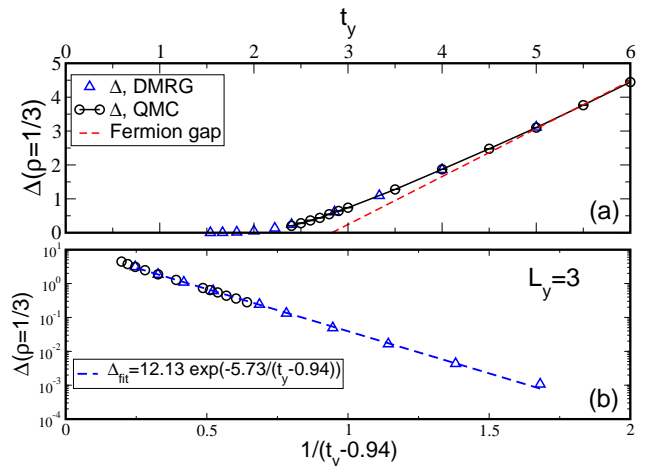


FIG. 3: (Color online) (a) The gap Δ at $\rho = \frac{1}{3}$ in a three-leg ladder as a function of t_y . The values of Δ are extrapolated from lattice sizes up to $L_x = 250$. For large t_y , Δ approaches the value appropriate for a collection of noninteracting fermions (dashed red line). (b) Semilogarithmic plot of the gaps in (a) as a function of $1/(t_y - 0.94)$.

The dependence of the bosonic gap on t_y at $\rho = \frac{1}{3}$ in a three-leg system is shown in Fig. 3(a). The gap $\Delta(N)$ is computed from the jump in the chemical potential $\mu(N) = E(N) - E(N-1)$ at the critical density, i.e. $\Delta(N) = \mu(N+1) - \mu(N) = E(N+1) + E(N-1) -$

$2E(N)$. We use both the ALPS SSE and DMRG codes. The results are extrapolated using lattice sizes up to $L_x = 250$ for the smaller values of the gap. In the DMRG calculations we keep 800 states, which we have verified to be converged. The gap for a noninteracting three-leg fermion chain is also presented. The convergence of the bosonic results to the fermionic ones at large t_y suggests a fermion mapping is appropriate even in the absence of a formal Jordan-Wigner transformation. The boson Δ is larger than its fermionic counterpart and is unambiguously non-zero below the critical t_y where fermions would become metallic. A key issue is whether finite Δ persists all the way down to $t_y = 0$ as occurs for the two-chain case¹⁸.

To try to answer this question, Fig. 3(b) shows a semilogarithmic plot of the gap as a function of $1/(t_y - t_y^c)$ where t_y^c is the putative critical value at which the gap vanishes. A fit of the form $\Delta = a \exp(-b/(t_y - t_y^c))$ yields $t_y^c \approx 0.94$ and this is shown as the dashed (blue) line in the lower panel. In the two-chain case, Crepin *et al.* have found¹⁸ an exponential behavior all the way to very small (vanishing) t_y (large $1/t_y$). As a consequence, they argued that an exponentially small gap persists all the way to $t_y = 0$. In the present three-leg case, the evidence for a finite value for t_y^c is clear. The value is considerably less than the fermionic band structure value $4/\sqrt{2}$ and even suggests that when the system is isotropic, $t_x = t_y$, the three-leg system is gapped at $\rho = \frac{1}{3}$ (and also $\rho = \frac{2}{3}$).

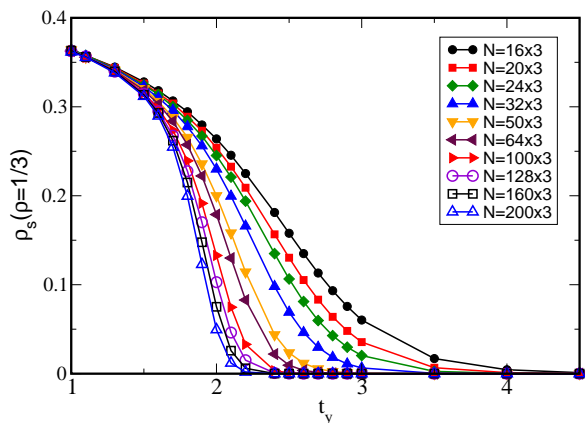


FIG. 4: (Color online) SF density at $\rho = \frac{1}{3}$ as a function of t_y . The SF density remains nonzero for small t_y , even in the largest lattice size we study here.

To confirm the above result for t_y^c , we turn to an examination of the SF density at $\rho = \frac{1}{3}$ to see if it becomes nonzero at finite, small t_y . Figure 4 shows ρ_s at $\rho = \frac{1}{3}$ for lattice sizes $L_x = 16$ to $L_x = 200$. The SF density decreases with increasing t_y , and for $t_y \gtrsim 4/\sqrt{2}$, the fermionic critical value for the three-band case previously discussed, the behavior seems unambiguously

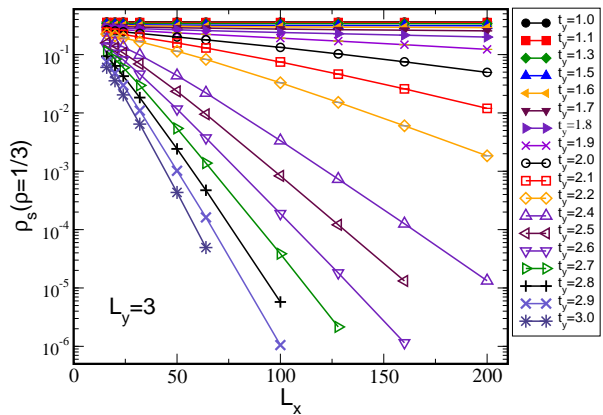


FIG. 5: (Color online) Semilogarithmic plot of the SF density at $\rho = \frac{1}{3}$ for different t_y , as a function of L_x . In a non-SF phase, we expect $\rho_s \sim \exp(-L_x/\xi)$ and hence linear behavior here.

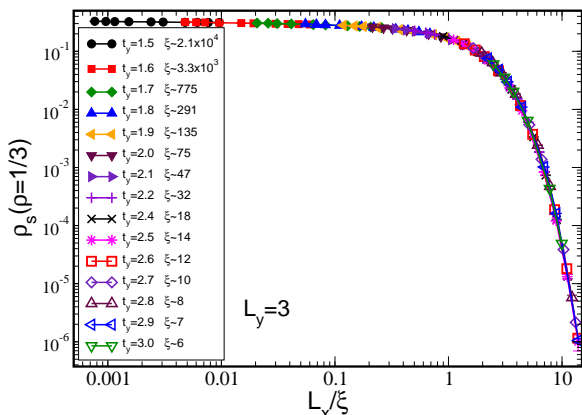


FIG. 6: (Color online) Collapse of the data in Fig. 5, by rescaling the x axis, from $L_x \rightarrow L_x/\xi$, with the correlation length ξ obtained from Fig. 5.

insulating ($\rho_s = 0$), consistent with the analysis of the charge gap. Indeed ρ_s vanishes even for somewhat smaller t_y , in agreement with the observation that the bosonic charge gap lies above the fermion one. However, for smaller t_y , the SF density is nonzero even for the largest lattice size we consider here.

The persistence of nonzero ρ_s as the lattice size increases in Fig. 4 can be taken as an indication of a nonzero t_y^c . To verify this possibility quantitatively, we make a semilogarithmic plot of the SF density versus L_x for different t_y (Fig. 5). For large t_y , the SF density decays exponentially with L_x and we can compute correlation length $\xi(t_y)$ from $\rho_s \simeq \exp(-L_x/\xi)$. This

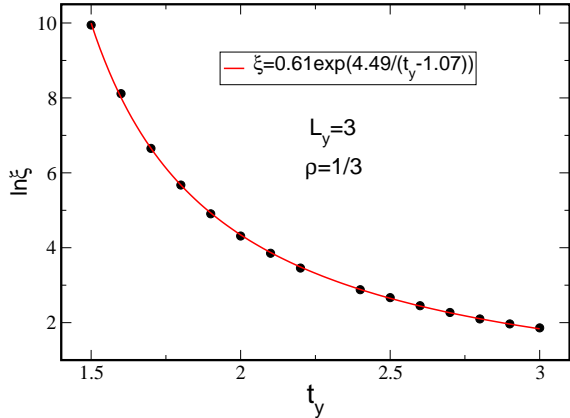


FIG. 7: (Color online) Correlation length ξ of the three-leg ladder versus the \hat{y} direction hopping t_y . The points obtained from the data collapse (black circles) are well fitted by the exponential form (red curve).

analysis parallels that presented in [18]. The values of ξ are presented in the legend of Fig. 6. They are fairly well determined down to $t_y \sim 1.7$ where ξ is still on the order of the size of our simulation box. For smaller t_y the correlation length becomes much larger than L_x , as indicated by the nearly horizontal traces in Fig. 5. A consistency check on our extraction of ξ is provided by collapsing the data for ρ_s , that is, via plotting results for different t_y as a function of a rescaled horizontal axis L_x/ξ as in Fig. 6.

Figure 7 provides a fit of these values of ξ to the functional form $\xi = \xi_0 \exp[a/(t_y - t_y^c)]$. The best fit is obtained for $t_y^c \approx 1.07$. This value is in good agreement with the value, $t_y^c \approx 0.94$, obtained above from a study of the charge gap and confirms that a finite, but not very large, value of the transverse hopping, t_y , is necessary to establish a gapped insulating phase at $\rho = \frac{1}{3}$.

In Fig. 8, we investigate the individual components of the energy. The kinetic energy is maximized (in absolute value) at half filling, because we are studying the case with no intersite interactions. For $t_y = 1$, all the energy curves are smooth; for $t_y = 6$, the curves of potential energy and total energy have vertical jumps at $\rho = \frac{1}{3}$ and $\frac{2}{3}$, which correspond to the insulating gap in Fig. 2. The curve of the kinetic energy also has kinks at those densities, although these are barely visible at the scale of the figure.

Figure 9 is the same as Fig. 2 but for the four-leg ladder and shows (a) the density as a function of chemical potential for a system of 64×4 sites. Plateaux are seen to develop at $\rho = \frac{1}{4}, \frac{1}{2}, \frac{3}{4}$ for sufficiently large t_y . Figure 9(b) shows the SF density, and confirms that it vanishes in the gapped phase. In this case the fermionic band structure consists of four bands (two of which are degenerate) with $\epsilon(\mathbf{k}) = -2t_x \cos k_x + 2t_y \{-1, 0, 0, +1\}$, and the fermionic

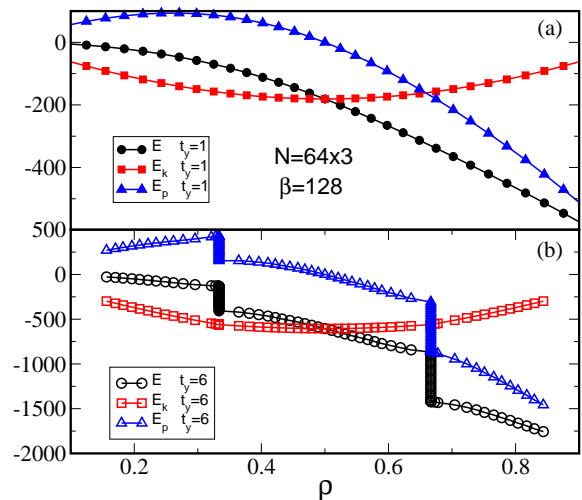


FIG. 8: (Color online) Kinetic, potential, and total energies of the three-leg ladder as functions of the filling ρ for (a) $t_y = 1$ and (b) $t_y = 6$. The kinetic energy is maximized (in absolute value) at half filling. While all the energy curves are smooth for $t_y = 1$, for $t_y = 6$ the curves of potential energy and total energy have vertical jumps at $\rho = \frac{1}{3}$ and $\frac{2}{3}$, also displayed by the kinetic energy although barely visible on the scale of the figure.

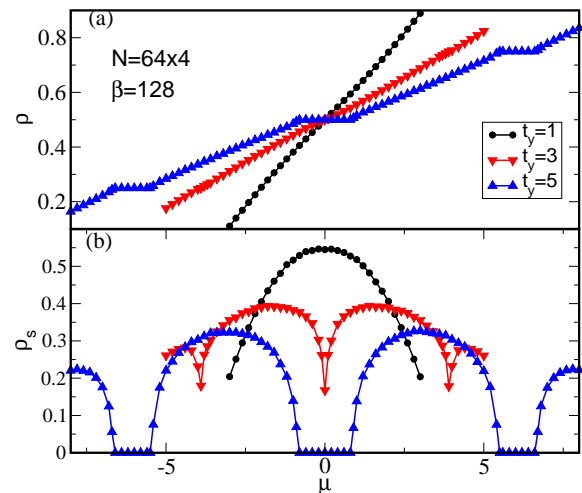


FIG. 9: (Color online) (a) $\rho(\mu)$ and (b) SF density for a four leg ladder of hard-core bosons, similar to those in Fig. 2. As the transverse hopping t_y grows, gaps develop at $\rho = \frac{1}{4}, \frac{1}{2}, \frac{3}{4}$, and SF density vanishes there.

gaps $\Delta_f(\rho = \frac{1}{4}) = \Delta_f(\rho = \frac{3}{4}) = t_y - 4$, $\Delta_f(\rho = \frac{1}{2}) = \sqrt{2(3 - \sqrt{5})}t_y - 4$. As opposed to Fig. 2 which showed two gaps between the three bands, we have here three gaps at $\rho = \frac{1}{4}, \frac{1}{2}, \frac{3}{4}$ between the four bands.

Figures 10 and 11 show in the (a) panels gaps at $\rho = \frac{1}{4}$ and $\rho = \frac{1}{2}$ respectively as functions of t_y for the four-leg lattice, similar to Fig. 3. As for the three-leg ladder, these gaps are obtained with DMRG and QMC using the

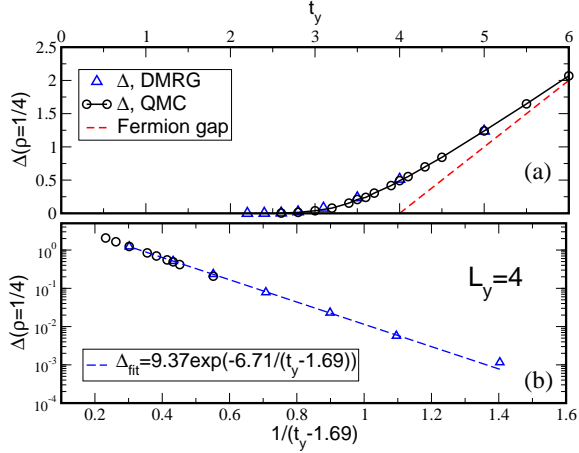


FIG. 10: (Color online) (a) The extrapolated gaps at $\rho = \frac{1}{4}$ in the four-leg ladder as a function of t_y from QMC and DMRG. (b) Semilogarithmic plot of the gap versus $(t_y - 1.69)^{-1}$. Exponential decay over three decades is seen giving the critical value $t_y^c \approx 1.69$.

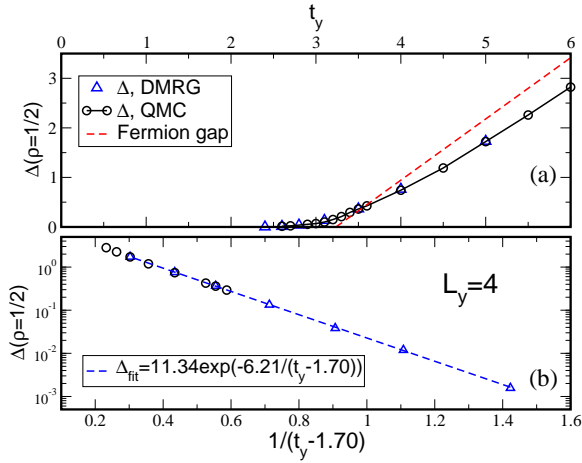


FIG. 11: (Color online) (a) The extrapolated gaps at $\rho = \frac{1}{2}$ in the four-leg ladder as a function of t_y from QMC and DMRG. (b) Semilogarithmic plot of the gap versus $(t_y - 1.70)^{-1}$. Exponential decay over three decades is seen giving the critical value $t_y^c \approx 1.70$.

definition $\Delta(N) = E(N+1) + E(N-1) - 2E(N)$ and then extrapolated from lattice sites $L_x = 16$ to 128 (with DMRG L_x is taken up to 250). The fermionic gaps are also included in these figures. Compared with the three-leg ladder, the gaps in the four-leg system need somewhat larger t_y to form and, as expected, the gaps at $\rho = \frac{1}{2}$ are wider than at $\rho = \frac{1}{4}$. The fermionic band gaps provide a reasonable estimate of those seen in the bosonic case.

We have also examined the exponential behavior of the gap at $\rho = \frac{1}{4}$ and $\rho = \frac{1}{2}$ in the four-leg ladder as

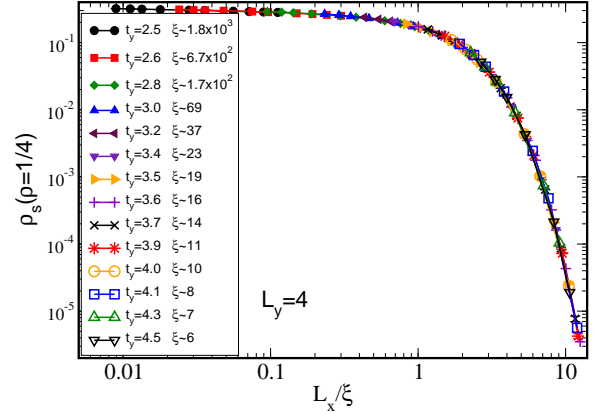


FIG. 12: (Color online) The SF density, ρ_s , versus the scaled system size, L/ξ . ξ is the correlation length at the values of t_y shown in the legend. These values of ξ are used in Fig. 13 to obtain the critical value of the hopping, t_y^c .

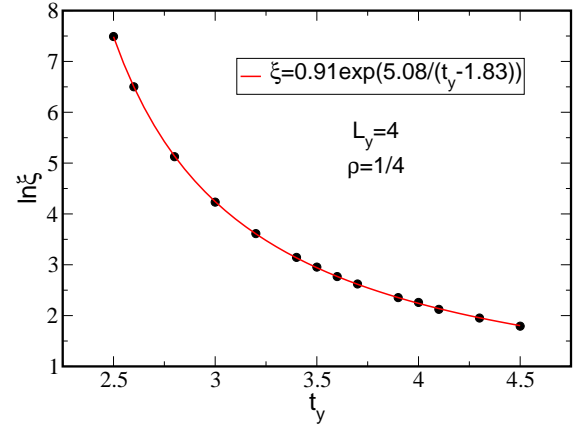


FIG. 13: (Color online) Correlation length at $\rho = \frac{1}{4}$ for the four-leg ladder versus the transverse hopping t_y . The points obtained from the data collapse (black circles) are fitted well by the exponential form (red curve) indicating a finite critical value $t_y^c \approx 1.83$.

described for the three-leg system. The (b) panels of Figs. 10 and 11 show semilogarithmic plots of the gaps as functions of $(t_y - t_y^c)^{-1}$ with $t_y^c = 1.69$ for $\rho = \frac{1}{4}$ and $t_y^c = 1.70$ for $\rho = \frac{1}{2}$. Exponential decay is seen over three decades yielding finite values for the critical hoppings. As in the three-leg case the critical values of t_y at which gaps appear are reduced from their fermion counterparts.

As for the three-leg ladder, we confirm the above results for t_y^c by examining the SF density at $\rho = \frac{1}{4}$ and $\rho = \frac{3}{4}$ to see if it becomes nonzero at finite, small t_y . The lattice size is up to $L_x = 200$, as in the three-leg case

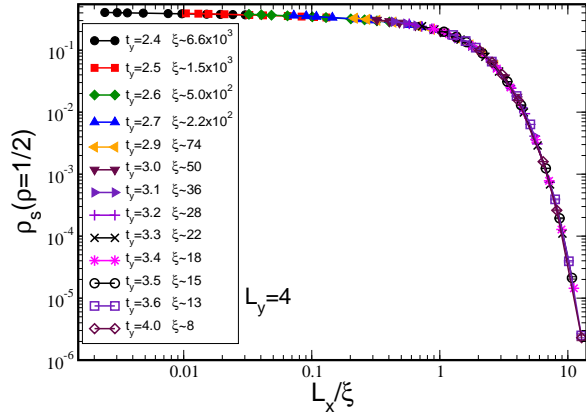


FIG. 14: (Color online) As in Fig. 12 but for $\rho = \frac{1}{2}$. The values of ξ are used in Fig. 15 to obtain the critical value of the hopping, t_y^c .

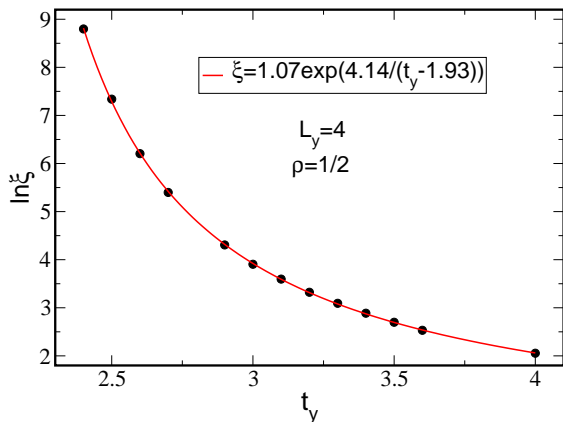


FIG. 15: (Color online) Correlation length at $\rho = \frac{1}{2}$ of the four-leg ladder versus the transverse hopping t_y . The points obtained from the data collapse (black circles) are fitted well by the exponential form (red curve). This gives the finite critical value for the hopping, $t_y^c \approx 1.93$.

(Fig. 4). We follow the same analysis which led to Figs. 4 and 5 but only show figures for the scaled SF density. Figure 12 gives, for $\rho = \frac{1}{4}$, ρ_s versus the scaled size of the system, L_x/ξ , where ξ is the correlation length at the various values of t_y shown in the legend of the figure. The data collapse is excellent and the values of ξ thus obtained are shown versus t_y in Fig. 13. The exponential fit, also shown in the figure, yields the critical value $t_y^c = 1.83$, which is in reasonable agreement with the value obtained from the gap, $t_y^c = 1.69$. Figures 14 and 15 show the corresponding figures at $\rho = \frac{1}{2}$ and yield $t_y^c = 1.93$ in

good agreement with the value obtained directly from the gaps, $t_y^c = 1.70$.

IV. CONCLUSIONS

The most simple physical picture of the origin of Mott insulating phases focuses on the (large) repulsive interaction energy, and the filling at which the addition of quantum particles first causes that energy to appear. In a model with only a strong on-site repulsion, particles can be added without any potential energy cost up until a commensurate filling one particle per site. At that point, double occupancy becomes unavoidable, and the cost to increase the density jumps. The precise form of the kinetic energy, e.g., whether it is isotropic in different spatial directions, or connects only near-neighbor sites, is irrelevant to this simplistic argument: As long as any empty sites remain in the lattice there is no charge gap and, at low temperatures, a collection of bosonic particles will form a SF phase. However, recent work by Crepin has demonstrated that in two-leg ladders insulating phases can arise at half-filling, underlining the need to refine this picture.

In this paper we studied hard-core bosons in three- and four-leg ladders with anisotropic hopping parameters in the \hat{x} and \hat{y} directions, t_x and t_y . To this end, we used both QMC and DMRG from the ALPS library¹⁹. Our focus was the possibility of the appearance of gaps at fractional fillings as happens for the two-leg ladder¹⁸, a possibility which seems surprising in light of the argument above. At the other extreme, when the number of coupled chains is large and the system approaches the limit of a two-dimensional system, one expects gaps to appear at fractional fillings but at very large values of t_y/t_x ²⁵. We have shown above that for both the three-leg and the four-leg systems gaps appear at values of t_y/t_x , which are smaller than those resulting from an argument based on fermionic bands. While in the case of the two-leg system, the gap at $\rho = \frac{1}{2}$ persists¹⁸ all the way down to $t_y = 0$, we found that, in the three-leg case, a gap appears at $\rho = \frac{1}{3}$ starting at the isotropic value, $t_y/t_x \approx 1$. For the four-leg system, a gap at $\rho = \frac{1}{4}$ appears starting at $t_y/t_x \approx 1.8$ and for $\rho = \frac{1}{2}$ at $t_y/t_x \approx 1.9$.

ACKNOWLEDGMENTS

This work was supported by: the National Key Basic Research Program of China (Grant No. 2013CB328702), the National Natural Science Foundation of China (Grant No. 11374074), a CNRS-UC Davis EPOCAL LIA joint research grant, and by the University of California Office of the President. We thank J. McCrea for useful input.

-
- ¹ D. Jaksch, C. Bruder, J.I. Cirac, C.W. Gardiner, and P. Zoller, *Phys. Rev. Lett.* **81**, 3108 (1998).
- ² G.-B. Jo, J. Guzman, C. K. Thomas, P. Hosur, A. Vishwanath, and D. M. Stamper-Kurn, *Phys. Rev. Lett.* **108**, 045305 (2012).
- ³ D. Greif, T. Uehlinger, G. Jotzu, L. Tarruell, and T. Esslinger, *Science* **340**, 1307 (2013).
- ⁴ M.P.A. Fisher, P.B. Weichman, G. Grinstein and D.S. Fisher, *Phys. Rev.* **B 40**, 546 (1989).
- ⁵ B. Capogrosso-Sansone, S.G. Söyler, N. Prokof'ev, and B. Svistunov, *Phys. Rev.* **A77**, 015602 (2008).
- ⁶ P. Niyaz, R.T. Scalettar, C.Y. Fong, and G.G. Batrouni, *Phys. Rev.* **B 44**, 7143 (1991).
- ⁷ B. Capogrosso-Sansone, C. Trefzger, M. Lewenstein, P. Zoller, and G. Pupillo, *Phys. Rev. Lett.* **104**, 125301 (2010).
- ⁸ T. Ohgoe, T. Suzuki, and N. Kawashima, *Phys. Rev.* **A86**, 063635 (2012).
- ⁹ P. Buonsante, V. Penna, A. Vezzani, *Phys. Rev.* **A70**, 061603R (2004).
- ¹⁰ P. Buonsante, A. Vezzani, *Phys. Rev.* **A72**, 013614 (2005).
- ¹¹ V.G. Rousseau, D.P. Arovas, M. Rigol, F. Hébert, G.G. Batrouni, and R.T. Scalettar, *Phys. Rev.* **B73**, 174516 (2006).
- ¹² P. Buonsante, V. Penna, and A. Vezzani, *Phys. Rev.* **A72**, 031602(R) (2005).
- ¹³ L. Santos, M. A. Baranov, J. I. Cirac, H.-U. Everts, H. Fehrmann and M. Lewenstein, *Phys. Rev. Lett.* **93**, 030601 (2004).
- ¹⁴ I. Danshita, J. E. Williams, C. A. R. Sá de Melo and C. W. Clark, *Phys. Rev.* **A76**, 043606 (2007).
- ¹⁵ I. Danshita, C. A. R. Sá de Melo and C. W. Clark, *Phys. Rev.* **A77**, 063609 (2008).
- ¹⁶ M. Girardeau, *J. Math. Phys.* **1**, 516 (1960).
- ¹⁷ P. Jordan and E. Wigner, *Z. Phys.* **47**, 631 (1928).
- ¹⁸ F. Crepin, N. Laflorencie, G. Roux, and P. Simon, *Phys. Rev.* **B 84**, 054517 (2011).
- ¹⁹ B. Bauer, L. D. Carr, H.G. Evertz, A. Feiguin, J. Freire, S. Fuchs, L. Gamper, J. Gukelberger, E. Gull, S. Guertler, A. Hehn, R. Igarashi, S.V. Isakov, D. Koop, P.N. Ma, P. Mates, H. Matsuo, O. Parcollet, G. Pawłowski, J.D. Picon, L. Pollet, E. Santos, V.W. Scarola, U. Schollwöck, C. Silva, B. Surer, S. Todo, S. Trebst, M. Troyer, M.L. Wall, P. Werner, and S. Wessel, *J. Stat. Mech.* (2011) P05001.
- ²⁰ A. W. Sandvik, *Phys. Rev.* **B 59**, 14157 (1999).
- ²¹ F. Alet, S. Wessel, and M. Troyer, *Phys. Rev.* **E 71**, 036706 (2005).
- ²² L. Pollet, S. M. A. Rombouts, K. Van Houcke, and K. Heyde, *Phys. Rev.* **E 70**, 056705 (2005).
- ²³ D.C. Handscomb, *Proc. Cambridge Philos. Soc.* **58**, 594 (1962).
- ²⁴ E.L. Pollock and D.M. Ceperley, *Phys. Rev.* **B30**, 2555 (1984); D.M. Ceperley and E.L. Pollock, *Phys. Rev. Lett.* **56**, 351 (1986); and E.L. Pollock and D.M. Ceperley, *Phys. Rev.* **B36**, 8343 (1987).
- ²⁵ T. Ying, G.G. Batrouni, V.G. Rousseau, M. Jarrell, J. Moreno, X.D. Sun, and R.T. Scalettar, *Phys. Rev.* **B 87**, 195142 (2013).